Published in final edited form as:
Clin Cancer Res. 2009 January 15; 15(2): 597–606. doi:10.1158/1078-0432.CCR-08-1277.

Invariant natural killer T cells regulate breast cancer response to radiation and CTLA-4 blockade

Karsten A. Pilones[1], **Noriko Kawashima**[1], **Anne Marie Yang**[1], **James S. Babb**[2], **Silvia C. Formenti**[3], and **Sandra Demaria**[1,4]

[1]Department of Pathology, New York University School of Medicine and NYU Langone Medical Center, New York, NY, 10016.

[2]Department of Radiology, New York University School of Medicine and NYU Langone Medical Center, New York, NY, 10016.

[3]Department of Radiation Oncology, New York University School of Medicine and NYU Langone Medical Center, New York, NY, 10016.

Abstract

Purpose—Immunoregulatory and suppressive mechanisms represent major obstacles to the success of immunotherapy in cancer patients. We have shown that the combination of radiotherapy (RT) to the primary tumor and CTLA-4 blockade induces anti-tumor immunity inhibiting metastases and extending the survival of mice bearing the poorly immunogenic and highly metastatic 4T1 mammary carcinoma. Similarly to patients with metastatic cancer, however, mice were seldom cured. Here we tested the hypothesis that invariant natural killer T (iNKT) cells, a subset with unique regulatory functions, can regulate the response to RT and CTLA-4 blockade.

Experimental design—Growth of 4T1 primary tumors and lung metastases was compared in wild type (WT) and iNKT cells-deficient (iNKT−/−) mice. Treatment was started on Day 13 when the primary tumors were palpable. Mice received RT to the primary tumor in two doses of 12 Gy in combination or not with 9H10 mAb against CTLA-4. Response to treatment was assessed by measuring primary tumor growth delay/regression, survival, and number of lung metastases.

Results—The response to RT+9H10 was markedly enhanced in the absence of iNKT cells, with 50% of iNKT−/− *versus* 0% of WT mice showing complete tumor regression, long-term survival, and resistance to a challenge with 4T1 cells. Administration of the iNKT cell activator α-galactosylceramide did not enhance the response of WT mice to RT+9H10. Tumor-infiltrating iNKT cells were markedly reduced in WT mice treated with RT+9H10.

Conclusions—iNKT cells play a major role in regulating the response to treatment with local RT and CTLA-4 blockade.

Keywords

NKT cells; breast cancer; metastases; CTLA-4 blockade; radiotherapy

4Correspondence and reprint requests should be addressed to Sandra Demaria, Department of Pathology, MSB-504, New York University School of Medicine, 550 First Avenue, New York, NY 10016. Phone: (212) 263-7308; Fax (212) 263-8211; E-mail: demars01@med.nyu.edu.

INTRODUCTION

Pre-clinical models and clinical trials have provided the proof of principle that immunotherapy (IT) can treat cancer (reviewed in reference 1). However, despite the development of multiple vaccination strategies to induce anti-tumor T cells, objective responses are seen only in a small fraction of patients and it remains unclear what are the factors that determine the success of any given treatment. Increased understanding of the complex networks of immune cells and cytokines that control immune system function has led to the identification of several regulatory and suppressive mechanisms as major obstacles to the success of IT (2). These are of two types, tumor-induced and pre-existing in the host as the result of genetic predisposition, age, concurrent diseases or previous therapies (3). Myeloid-derived suppressor cells (MDSC) (4), belong to the first category since their accumulation in tumor-bearing mice and cancer patients is driven by tumor growth (5). Regulatory T cells (T-regs) play a key role in the maintenance of self tolerance as well as tolerance to tumors (6). Natural Tregs develop in the thymus and belong to the second category (7). In contrast, adaptive Tregs are generated in the periphery from mature T cells and their differentiation is induced by the tumor microenvironment (8,9).

Another T cell subset with regulatory function, natural killer T (NKT) cells, has been implicated in both up- and down-regulation of immune responses (10). NKT cells have unique properties in that they can rapidly produce both Th1 and Th2 cytokines upon activation and function as a powerful switch to turn on or off the innate and adaptive immune response in various diseases and conditions (10–12). NKT cells recognize glycolipid antigens presented by CD1d molecules, and in mice most express a canonical α-chain (Vα14Jα18), and are known as invariant (iNKT) or type I NKT cells. In humans, the homologous population of iNKT cells expresses Vα24 (10). iNKT cells react with α-galactosylceramide (αGC), a synthetic CD1d-binding glycolipid that has a strong agonistic activity, whereas the non-invariant or type II NKT cells, although restricted by CD1d, do not bind αGC (13).

In cancer, NKT cells have been associated with spontaneous immunosurveillance in some experimental systems (14,15) but have been shown to suppress immunosurveillance in others (16,17). Recent work by Terabe *et al.*, (18) suggests a functional difference between the two subsets of NKT cells in regulation of anti-tumor immunity, with type II NKT cells being mostly responsible for immunosuppression. An immunoregulatory pathway that links the production of Interleukin (IL)-13 by NKT cells to induction of TGFβ production by MDSC has been shown to be responsible for the inhibition of anti-tumor CTL that results in tumor recurrence in some tumor models (16,19,20) but not others (21,22). Overall, the mechanisms of NKT cell-mediated immunoregulation in cancer involve multiple pathways and remain largely undefined.

Activation of iNKT cells by systemic administration of αGC to mice and humans has been shown to induce the rapid production of Interferon (IFN)-γ and IL-4 and other Th1 and Th2 cytokines (10). Importantly, in several pre-clinical cancer models this resulted in effective anti-tumor immunity mediated by the downstream activation of antigen-presenting cells (APC), NK and CD8+ T cells (23). However, in initial clinical trials αGC has not shown significant anticancer activity, possibly due to partially impaired NKT cell function in cancer patients (24).

Accumulated evidence in experimental models supports the development of a novel therapeutic approach based on the combination of ionizing radiation therapy (RT) with IT for the treatment of cancer (reviewed in references 25 and 26). In most cases clinical trials testing the efficacy of novel treatments are performed in patients with advanced stage disease, a population for which the need for new therapies is most urgent, but that also presents with an immunological environment largely altered by the tumor. To mimic this situation, we have employed as a model the poorly immunogenic 4T1 mouse mammary carcinoma. After s.c. inoculation 4T1

cells grow to form a highly invasive primary tumor that early on sheds spontaneous metastases to the lungs, and other organs (27). Mice usually die of metastatic disease to the lungs. We previously tested the combination of RT with CTLA-4 blockade approximately two weeks after implantation in mice, when primary tumors are palpable and metastatic cells have already spread systemically (28). Whereas single modality treatment was ineffective, the combination of local RT to the primary tumor and CTLA-4 blockade elicited CD8 T-cell-dependent anti-tumor immunity. The immune response effectively inhibited the growth of spontaneous lung metastases prolonging the survival time of animals. However, cure was rare, and most mice eventually succumbed to their disease (28).

In this study we investigated whether the disruption of immunoregulatory circuits can improve the response to treatment with RT and CTLA-4 blockade. Our data indicate that whereas 4T1 tumors grew equally well in wild type (WT) mice and mice lacking iNKT cells (iNKT−/−), the latter developed a CD8 response that partially inhibited metastases but not primary tumor growth. This observation is in agreement with a minor role of iNKT cells in regulating spontaneous immunosurveillance in the 4T1 model (18). Remarkably, as compared to WT mice, iNKT−/− mice showed a marked improvement in survival and cure rate following treatment with RT and CTLA-4 blockade, suggesting that iNKT cells can play a major role in regulating the response to treatment. Administration of αGC did not improve the response of WT mice to RT and CTLA-4 blockade. Despite the differential response to treatment WT and iNKT−/− mice showed a similar systemic and intra-tumoral increase in MDSC around the time treatment was started, suggesting that the degree of MDSC accumulation does not predict the response to treatment.

MATERIALS AND METHODS

Mice

Six to eight week old BALB/c mice were obtained from Taconic Animal Laboratory (Germantown, NY). iNKT−/− (Vα14 Jα18-deficient) mice (29) in the BALB/c background obtained from M. Taniguchi (RIKEN Research Center for Allergy and Immunology, Yokohama, Kanagawa, Japan), were bred at New York University and used between 6 and 12 weeks of age. All experiments were approved by the Institutional Animal Care and Use Committee of New York University.

Cells and reagents

4T1 is a BALB/c mouse-derived mammary carcinoma cell line (provided by Fred Miller, the Michigan Cancer Center, Detroit, MI, reference 27) and A20 is a BALB/C mouse-derived B-cell leukemia/lymphoma (30). 4T1 cells were grown in DMEM medium (Invitrogen Corporation, Carlsbad, CA) supplemented with 2mM L-glutamine, 100 U/ml penicillin, 100 μg/ml streptomycin, 2.5×10^{-5} M 2-mercapthoethanol, and 10% FBS (Gemini Bio-Products Woodland, CA) (complete medium). These cells were found to be free of contamination by Mycoplasma by the Mycoplasma detection kit (Roche Diagnostics, Chicago, IL). Anti-CTLA-4 hamster mAb 9H10 was purified as previously described (28). Control hamster IgG was purchased from Jackson Immunoresearch Laboratories (West Grove, PA). Purified anti-CD4 (GK1.5), anti-CD8 (2.43) rat mAb and control rat IgG were purchased from BioExpress, Inc. (West Lebanon, NH).

Tumor challenge and treatment

Mice were injected s.c. in the right flank with 5×10^4 4T1 cells in 0.1 ml of DMEM medium without additives on Day 0. Perpendicular tumor diameters were measured with a Vernier caliper, and tumor volumes were calculated as length × width^2 × 0.52. On Day 13, when tumors reached the average diameter of 5 mm (approximately 65 mm^3 in volume) animals were

randomly assigned to various treatment groups, as indicated. RT was administered as previously described (28). Briefly, all mice (including mice receiving mock radiation) were lightly anesthetized by i.p. injection of Avertin (240mg/kg), positioned on a dedicated plexiglass tray and the whole body was protected by lead shielding, except for the area of the tumor to be irradiated. RT was delivered to a field including the tumor with 5 mm margins using a ^{60}CO radiation source by two fractions of 12 Gy each on Days 13 and 14. Control hamster IgG and 9H10 were given i.p. at 200 μg at 1, 4 and 7 days after RT. α-GC (Alexis Biochemicals, San Diego CA) was dissolved in DMSO and diluted in PBS supplemented with 0.5% polysorbate-20 (w/v) prior to injection and given i.p. at 100 ng/mouse twice a week, starting on Day 1 post-RT. Tumor growth was evaluated every 2 to 3 days until death or sacrifice when tumor dimensions exceeded 5% body weight or mice showed dyspnea, abnormal posture, >20% body weight loss, difficulty with ambulation or any other clinical sign of metastatic disease causing significant pain or distress, according to institutional guidelines. In some experiments, mice that rejected the tumors and survived tumor free until Day 120 were injected in the controlateral flank with a tumorigenic inoculum of either 4T1 or A20 cells and followed for up to 60 days for tumor development.

Clonogenic lung metastases assay

For determination of the number of clonogenic lung metastases, lungs were harvested at Day 33 or 35 post s.c. injection in the right flank with 5×10^4 4T1 cells and processed as previously described (27). Briefly, lungs from each individual animal were minced into 1 mm pieces, and digested with 5 ml enzyme cocktail containing 1mg/ml Collagenase IV and 6 units/ml elastase, both from Sigma Chemical Company (St Louis, MO) in PBS for 1 h at 4°C with rotation. Cell suspensions were filtered through 70-μm nylon cell strainers and washed two times with HBSS, then resuspended in complete medium. Serial 3 to 5-fold dilutions were plated in 10-cm tissue culture dishes in the presence of 60μM 6-thioguanine (2-amino-6-mercaptopurine, Sigma Chemical Company, St Louis, MO) to allow only the growth of 4T1 cells which are resistant to this drug (27). When colonies of growing 4T1 cells became visible (8 to 14 days) the plates were washed with PBS, fixed with methanol, and stained with Crystal violet. The colonies were counted independently by 2 to 3 investigators, blinded to the group to which each mouse belonged, and the total number/lungs was calculated for each animal.

In vivo T-cell subset depletion

Depletion of CD4 and CD8 T-cell subsets was performed by injecting GK1.5 or 2.43 mAb i.p. at 100 μg/mouse on three consecutive days, starting one day before the s.c. injection in the right flank with 5×10^4 4T1 cells. The depletion was maintained by repeated weekly injections of mAb. Depletion was confirmed by testing spleen cells from control animals for the presence of CD4 and CD8 T-cells using non-cross-reactive FITC-RMA4-4 and PE-anti-CD8β mAb (BD PharMingen, San Diego, CA).

Mice vaccination

WT and iNKT−/− mice were vaccinated with 10^6 irradiated (100 Gy) 4T1 cells s.c. in the right flank 3 times at weekly intervals. Control mice received DMEM. Seven days after the last vaccination mice were challenged with a tumorigenic inoculum (5×10^4) of 4T1 cells s.c. in the opposite flank and followed for tumor development.

Analysis of MDSC and iNKT cells infiltrating 4T1 tumors

The tumors were dissected carefully removing all surrounding normal tissue, minced into 1 mm pieces, and digested with collagenase D (400U/ml) for 25 minutes at 37 °C in a shaker. 10 ml of the enzyme solution were used for every *g* of tumor tissue. Obtained cell suspensions were filtered through 40-μm nylon cell strainers and washed two times with Hank's balanced

salt solution (HBSS). Aliquots of 10^6 tumor-derived cells were incubated with anti-mouse CD16/32 (Fc block) for 10 minutes followed by staining at 4°C with mAb against mouse Gr-1-Cy-Chrome and CD11b-PE (BD PharMingen, San Diego, CA) to identify MDSC, or with PE-conjugated mCD1d/PBS57 tetramer (provided by the NIH Tetramer Facility, reference 31) and FITC-conjugated CD3 to identify iNKT cells. Unloaded PE-conjugated mCD1d tetramer was used as control. Samples were analyzed using a FACScan flow cytometer and FlowJo version 6.4.4 (Tree Star, Ashland, OR).

Measurement of TGF β1 production

1×10^6 spleen cells from individual mice were cultured o.n. in RPMI 1640 medium supplemented with 1% FBS, 2mM L-glutamine, 100 U/ml penicillin, 100 μg/ml streptomycin in a 24-well plate. Supernatants were harvested and stored at −80°C. The concentration of TGF β1 was determined in duplicate samples using the Quantikine TGF β1 Immunoassay Kit (R&D Systems, Minneapolis, MN) following manufacturer's instructions. Background readings for culture medium were subtracted from all samples. As previously reported (19), acidification of the samples was required to detect the latent form of TGF β1 produced in vitro by MDSC.

Immunostaining of tumor sections

4T1 tumors from treated and untreated WT and iNKT$^{-/-}$ mice were harvested at Day 29 post tumor inoculation, fixed for 1 h at 4°C in 4% paraformaldehyde followed by overnight incubation in 30% sucrose, and frozen in OCT medium. Sections (8 μm) were incubated with 0.1% Tween-20 and 0.01% Triton-X100 for 20 minutes, followed by 4% rat serum in 4% BSA/PBS for an additional 30 minutes. Sections were stained with PE-Texas-Red-conjugated rat anti-mouse CD4 or PE-conjugated rat anti-mouse CD8α (Caltag, Carlsbad, CA), and counterstained with 5 μg/ml DAPI (Sigma). Images were obtained using a Nikon Eclipse 800 deconvolution microscope. Number of CD4 and CD8 T cells were counted in three randomly selected (20×) fields in each tumor.

Statistical analysis

ANOVA based on ranks was used to assess differences between animal groups defined by genotype and/or treatment received with respect to tumor weight, tumor volume or the number of lung metastases at a fixed time point. Specifically, each end point (tumor weight, tumor volume, number of metastases) was first converted to ranks within each experiment and the ranks were then used as the dependent variable in the analysis of variance. Ranks were used in place of the observed values to better satisfy underlying distributional assumptions. When the treatment groups constituted a 2×2 factorial design (presence/absence of CTLA-4 blockade/RT), the analysis examined the main effects for each treatment modality (RT, CTLA-4 blockade) and the interaction between the modalities. The log rank test was used to compare animal groups in terms of overall survival, defined as time to death or sacrifice. The median and mean survival times within each treatment arm were estimated using the Kaplan-Meier product-limit method and a 95% confidence interval for each median survival time was derived on the basis of a sign test. All reported p values are two-sided and were declared statistically significant at the 5% level. The statistical computations were carried out using SAS for Windows, version 9.0 (SAS Institute, Cary, NC).

RESULTS

iNKT−/− mice develop a spontaneous CD8-dependent anti-tumor immune response inhibiting metastases

To investigate the role of the host immune status in tumor growth and response to treatment we injected mice lacking iNKT cells with 4T1 cancer cells. Whereas primary tumors grew at

the same rate in iNKT−/− and WT mice (not shown) and primary tumor weight was not significantly different on Day 34 (mean±SD 1364 ±895 and 873±234 mg for iNKT−/− and WT mice, respectively; p=0.41) the number of metastatic cells in the lungs was significantly lower in iNKT−/− mice (mean±SD: 525.4±1461.9, 1364.0±895.5 for iNKT−/− and WT, respectively; p=0.0009) (Figure 1A). The depletion of CD8 T cells or CD4 and CD8 T cells abrogated the difference in lung metastases between WT and iNKT−/− mice, whereas the depletion of CD4 T cells did not have any effect, indicating that CD8 T cells are required for the inhibition of lung metastases observed in iNKT−/− mice (Figure 1B). Interestingly, primary tumor growth was not affected by depletion of CD8 or CD4 T cells but a statistically significant increase in tumor weight ($p<0.01$) was seen in double depleted mice (Figure 1C).

The spontaneous development of anti-tumor CD8 T cells could be due to increased intrinsic immunogenicity of 4T1 cells in iNKT−/− mice. To test this hypothesis WT and iNKT−/− mice were immunized repeatedly with 4T1 cells inactivated by irradiation, followed 7 days after the last immunization by challenge with 5×10^4 live 4T1 cells. If anti-tumor CD8 cells had developed following vaccination, they would prevent or inhibit growth of the early small tumors. In contrast, all WT and iNKT mice developed tumors, and there was no significant difference between 4T1-vaccinated and non-vaccinated mice in tumor weight (Figure 1D). Therefore, 4T1 cells do not show increased immunogenicity in iNKT−/− mice.

In the absence of iNKT cells mice bearing established 4T1 mammary carcinoma show a markedly enhanced therapeutic response to treatment with local RT and CTLA-4 blockade

We have shown that WT mice bearing the poorly immunogenic 4T1 mammary carcinoma develop anti-tumor CD8 T cells inhibiting spontaneous lung metastases and extending their survival when treated with the combination of local RT to the primary tumor and CTLA-4 blocking mAb 9H10, whereas each single modality did not have an effect on survival (28). However, complete cure of the mice with well-established disease remained rare (0 to 15% of the mice were cured in different experiments (reference 28 and our unpublished results). This suggested that the duration and/or potency of the anti-tumor immune response elicited by treatment was limited in most animals. To test if iNKT cells play a role in response to treatment, iNKT−/− mice with established 4T1 tumors were randomly assigned to be treated with RT, CTLA-4 blockade or a combination of the two modalities. In the absence of treatment, tumors grew progressively, and all mice were dead by Day 49. RT alone was able to cause a significant ($p<0.05$) growth delay of the irradiated tumor, and complete regression in 2 out of 9 mice. Despite the fact that the growth of all irradiated tumors was delayed, there was no statistically significant improvement of survival (p=0.16) (Figure 2 A and B). This is consistent with the fact that RT as single modality cannot significantly inhibit the lung metastases outside of the field of radiation and, therefore, cannot extend survival, as previously observed in WT mice (28). However, the two iNKT−/− mice treated with RT alone that showed complete regression of the primary tumor remained tumor-free at Day 120, and demonstrated the development of a protective anti-tumor response, as described below.

iNKT−/− mice receiving CTLA-4 blocking mAb as single modality showed a significant, ($p<0.05$ from day 21 compared to control) though less pronounced than obtained with RT, tumor growth delay, and the tumor regressed completely in 1 out of 9 mice (Figure 2 A). This animal was cured of tumor, whereas the rest of the group showed a significant (p=0.002) but relatively modest increase in survival when compared to control group (Figure 2 B). This differs from results obtained in WT mice in which CTLA-4 blockade did not have any effect on primary tumor growth or survival (28).

Treatment with the combination of RT and CTLA-4 blockade caused complete regression of the irradiated tumor in 6 out of 9 mice (Figure 2 A and B), and a marked extension of their survival with all animals alive at Day 74 ($p<0.0001$ compared to control group). All tumor-

free mice that survived until Day 120 were considered “cured” and were rechallenged with a tumorigenic inoculum of 4T1 cells (2 mice in RT, 1 in 9H10, and 3 in RT+9H10 group) or the syngeneic but unrelated A20 lymphoma cells (3 mice in RT+9H10 group). All 6 mice rejected 4T1 tumor, whereas 5 of 5 naïve mice challenged at the same time developed tumors. In contrast, A20 tumor grew in the 3 survivor mice and 3 naïve mice (data not shown). These data indicate that iNKT−/− mice cured of tumor developed a long-lasting tumor-specific memory response.

To directly determine the effect of treatment on lung metastases, another experiment was performed in which tumor-bearing mice were treated as above and lungs analyzed at Day 35. Although single treatment with either RT or 9H10 showed a tendency to lower the number of metastatic cells, the difference was not statistically significant compared to control IgG-treated mice (Fig. 2 C). In contrast, mice treated with RT and CTLA-4 blockade showed complete inhibition of lung metastases (Fig. 2 C). The observation that RT’s effect on lung metastases was significant only in the presence of 9H10 is consistent with a synergism between RT and CTLA-4 blockade.

Next, responses to the combination treatment with RT and CTLA-4 blockade were directly compared between 4T1 tumor-bearing WT and iNKT−/− mice. In the absence of treatment, there was no difference in primary tumor growth between WT and iNKT−/− mice (Figure 3A). However, untreated iNKT−/− mice showed a small but statistically significant ($p=0.008$) (mean of 43.8 and 37.1 days for iNKT and WT mice, respectively) increase in survival. This is consistent with the CD8-mediated inhibition of metastases in iNKT mice (Figure 1).

Treatment with RT and CTLA-4 blockade initially caused a significant primary tumor growth delay in both WT and iNKT−/− mice, however, only iNKT−/− mice went on to achieve complete tumor regression and cure, as demonstrated by absence of tumor at Day 150, in 50% of the animals (Figure 3 A and B). None of the WT mice survived long-term, suggesting that only in iNKT−/− mice the duration and potency of the anti-tumor immune response was sufficient to completely eradicate the tumor.

Analysis of tumor infiltrating lymphocytes (TILs) at Day 29 showed that CD4+ cells were present in similar quantities in 4T1 tumors growing in WT and iNKT−/− mice, and were not significantly increased by treatment with RT and CTLA-4 blockade (Figure 3 C). In contrast, following treatment there was a significant increase in the number of CD8+ cells infiltrating 4T1 tumors in both WT and iNKT−/− mice ($p<0.01$ in treated versus untreated mice of both genotype) (Figure 3 D). Importantly, the number of CD8+ TILs was higher in iNKT−/− mice than in WT mice, and this difference was highly significant following treatment ($p=0.006$ in treated iNKT−/− versus treated WT mice). This data confirm our previous observations that CD8+ but not CD4+ T cells are responsible for 4T1 tumor inhibition induced by treatment with RT and CTLA-4 blockade (28, 32). In addition, they suggest that the anti-tumor response induced by treatment is stronger in the absence of iNKT cells.

The iNKT cell-specific activator αGC does not improve the response of tumor-bearing WT mice to treatment with RT and CTLA-4 blockade

αGC, a potent activator of iNKT cells, has been shown to induce powerful anti-tumor immune responses in several tumor models (23). Moreover, in a burn injury model, administration of αGC was able to prevent the immunosuppression that is mediated by iNKT cells (33). To determine whether administration of αGC to 4T1 tumor-bearing mice could activate iNKT cells to perform stimulatory rather than inhibitory functions, and improve the response of WT mice to RT and CTLA-4 blockade, mice were given αGC starting one day post-RT. αGC as a single modality did not have any effect on tumor growth, and it did not improve the tumor growth delay or survival caused by treatment with RT and RT + 9H10 (Figure 4 and data not

shown). However, a modest but statistically significant tumor growth delay was seen in mice treated with αGC and 9H10 (p=0.0396 compared to control vehicle-treated mice) (Figure 4).

Overall, these data indicate that administration of αGC to WT mice with established tumors does not improve their response to treatment with RT and CTLA-4 blockade.

Reduction in tumor-infiltrating iNKT cells after treatment with RT and CTLA-4 blockade

The presence within tumors of T cells with regulatory function has been shown to play an important role in suppression of anti-tumor immunity (8). To determine whether iNKT cells were present within 4T1 tumors growing in WT mice, cell suspensions prepared from 4T1 tumors and lungs were stained with CD3 and CD1d tetramers loaded with the αGC analog PBS-57 (31). In untreated mice iNKT cells represented ~4% of T cells infiltrating 4T1 tumors and 3% of T cells isolated from the lungs (Figure 5 A and B). Importantly, there was a pronounced decline in iNKT cells in both primary tumor and lungs following treatment with RT + 9H10 (Figure 5 B and C). Overall, these data indicate that iNKT cells are recruited to "primary" 4T1 tumors and their metastases, and that a treatment stimulating anti-tumor immunity leads to a relative decline in iNKT cell numbers, an observation that supports a regulatory role for iNKT cells.

WT and iNKT−/− mice do not differ in the tumor-driven expansion and recruitment of MDSC to tumors

Suppression of anti-tumor immune responses by NKT cells has been linked to their ability to induce TGFβ production by MDSC (19). To determine whether the markedly increased response to treatment in iNKT−/− mice was due to decreased accumulation of MDSC, the numbers of MDSC in the spleen and primary tumors of WT and iNKT−/− mice were analyzed on Day 14 of tumor growth, corresponding approximately to the time therapy was initiated. MDSC accumulation in spleens as well as primary tumors was similar between WT and iNKT −/− mice (Figure 6 A and B). Next, spleen cells of tumor-bearing WT and iNKT−/− mice were tested for secretion of TGFβ in short-term cultures. As previously reported for the 15-12RM tumor model (19) the secretion of TGFβ by spleen cells from 4T1 tumor-bearing WT mice was significantly increased compared to healthy mice ($p<0.05$). This was true also for cells derived from iNKT−/− mice (Figure 6 C). Although the baseline production of TGFβ did not differ significantly between WT and iNKT−/− healthy mice (p=0.35), tumor-bearing iNKT−/− mice produced more TGFβ than tumor-bearing WT mice, indicating that the production of TGFβ was not dependent on the presence of iNKT cells. Overall, these results are consistent with a recent report showing that NKT cells are not required to activate MDSC (34). They also indicate that the improved response to treatment with RT and CTLA-4 blockade seen in tumor-bearing iNKT−/− mice cannot be explained by differences in MDSC numbers or functional activation to produce TGFβ.

DISCUSSION

In this study, we show that mice lacking the iNKT cell subset and bearing well-established 4T1 tumors respond to treatment with the combination of local RT and CTLA-4 blockade with markedly increased overall survival and cure rate as compared to WT mice (Figure 2 and Figure 3 and reference 28). The improved response to treatment was not a result of increased immunogenicity of 4T1 cells in iNKT−/− mice since growth of the 4T1 tumors was similar in WT and iNKT−/− mice and vaccination with irradiated tumor cells did not induce a protective anti-tumor response (Figure 1D). However, iNKT−/− mice developed a spontaneous CD8 response inhibiting lung metastases (Figure 1).

The development of an anti-tumor immune response that is at least partially effective against metastases in face of a poorly immunogenic growing primary tumor is an example of concomitant tumor immunity (35). This well-known phenomenon is consistent with the notion that invasive cancers cause tissue damage and the generation of inflammatory signals attracting innate immune cells and eventually leading to the activation of the adaptive immune system (36). Treg have been shown to suppress concomitant immunity to the poorly immunogenic B16 melanoma (37). Our data suggest that iNKT cells play a similar role in case of the poorly immunogenic 4T1 carcinoma and are consistent with a previous observation that iNKT−/− mice have improved immunosurveillance against 4T1 metastases compared to WT mice (18). Importantly, whereas Terabi *et al.* (18) detected the immune response against metastases after surgical removal of the primary tumor, our work provides the evidence that it is generated in the absence of any surgical manipulation that could potentially contribute to the development of the anti-tumor response (38).

Treatment of iNKT−/− mice with local RT used as a single modality caused a reduction in lung metastases, that, however, was not statistically significant (Figure 2 C). Consistent with this, despite the complete "cure" obtained in ~20% of the mice, the effect of RT alone on survival was not significant (p=0.16) (Figure 1 B). This suggests that RT by itself was either not sufficient to induce a T cell response against this poorly immunogenic tumor, or that if induced it was suppressed (39). However, in combination with CTLA-4 blockade there was a highly significant anti-tumor effect leading to complete clearance of primary tumor and metastatic disease in over half of the mice (Figure 2 and 3). Overall, these data are consistent with the hypothesis that RT causes changes in the tumor microenvironment that can promote the afferent and efferent phases of the anti-tumor immune response (26, 32, 40).

CTLA-4 blockade used as a single modality had a modest but detectable effect in inhibiting tumor growth and extending the survival of iNKT−/− but not WT mice (Figure 2 and reference 28). This result was confirmed in two additional experiments (data not shown). CTLA-4 blockade used as a single treatment is known to be effective only against more immunogenic tumors in WT mice (41). This suggests that besides the intrinsic immunogenicity of a tumor, pre-existing host-specific factors can determine the response to CTLA-4 blockade. It is intriguing to consider whether the number or activity of iNKT cells could be a determinant of therapeutic responses mediated by anti-CTLA-4 antibodies in cancer patients (42).

Immunosuppression by NKT cells has been previously shown to be mediated by MDSC and TGFβ in some tumor models (16,19,20). In the 4T1 model, the increase in splenic MDSC in tumor-bearing mice was shown to correlate with the suppression of the immune response against metastases (43). Given the development of a spontaneous CD8 response inhibiting metastases in iNKT−/− mice, we expected to find less MDSC in iNKT−/− than in WT mice. In contrast, neither MDSC nor TGFβ production were reduced in the spleen of iNKT−/− mice (Figure 6). This suggests that MDSC likely exert their suppression locally, within the growing primary tumors, as previously shown by Kusmartsev *et al.* (44). In mice treated with RT, sensitization of CD11b+ MDSC by tumor-derived antigens that are released by radiation (40) could promote their destruction by anti-tumor CTL activated by anti-CTLA-4 antibodies leading to complete regression of established primary tumors.

Administration of the potent iNKT cell activator αGC did not improve the response of WT mice to treatment with local RT and CTLA-4 blockade (Figure 4). In a recent report, 4T1 tumor-bearing mice given αGC in a similar dose/schedule (100 ng every 4 days) in combination with anti-DR5 mAb to induce tumor cell apoptosis and anti-4-1BB mAb to provide costimulatory signals to T cells, showed significant rates of tumor rejection (45). This suggests that iNKT cell immunostimulatory function can be "rescued" by activation with αGC but the outcome of this activation is influenced by the immunological environment in which this takes

place. Indeed, αGC has been shown to promote iNKT cells regulatory functions when given to mice with autoimmune diseases (11). Therefore, it will be important to determine which IT strategies may be successfully combined with αGC to elicit anti-tumor immune responses in cancer patients.

It has been proposed that there is a dichotomy between the two main subsets of NKT cells, non-invariant (or type II) NKT cells being sufficient for negative regulation of the anti-tumor immune response, whereas iNKT cells are mostly responsible for protection (18). Our study shows that the selective absence of iNKT cells is sufficient to dramatically enhance the response to treatment with RT and CTLA-4 blockade in mice with an established metastatic mammary carcinoma. Importantly, at least in this tumor model, an anti-tumor immune response was detectable even in the absence of treatment, consistent with a role of iNKT cells in suppression of anti-tumor immunity. Therefore, it is likely that in cancer, similarly to other autoimmune/inflammatory diseases (10), the regulatory role of invariant and non-invariant NKT cells is not absolute, rather it is influenced by both the immunological environment of the tissue/tumor, and unknown factors of the host. For instance, a glycolipid produced by melanoma cells has been shown to be cross-presented by DC and to induce production of IL-10 by NKT cells (46). The presence of iNKT cells in 4T1 tumors (Figure 5) raises the question whether they may recognize a tumor-derived glycolipid. Few endogenous CD1d ligands are currently known. Identification of CD1d ligands that are expressed by cancer cells and may be recognized by different NKT cell subsets and/or with different affinity will help clarify the role of NKT cells in regulation of anti-tumor immunity (47).

Previous studies have shown a marked enhancement of anti-tumor immunity in CD1d-deficient mice that lack both subsets of NKT cells (18,21,22), and these results have been interpreted as evidence of a strong regulatory role of type II NKT cells. However, the recent evidence that some mouse tumors express low levels of CD1d (48), raises the possibility that CD1d may act as a neo antigen in CD1d-deficient mice, similarly to STAT6 in STAT6-deficient mice (49). Although CD1d expression in 4T1 cells has not been detected by immuno-staining and flow cytometry (reference 18 and data not shown), using a more sensitive technique, real time RT-PCR, we have found that 4T1 cells express CD1d (Supplementary Figure 1). Since CD1d-reactive T cells that may be present in the repertoire of CD1d-deficient mice, their possible role in 4T1 tumor rejection will need to be addressed.

In conclusion, we show that mice developing a detectable anti-tumor response to a syngeneic poorly immunogenic tumor because their regulatory circuits are “slightly” altered in the absence of the iNKT cells, only show a mild improvement in survival in the absence of treatment. However, their response to IT is dramatically improved in comparison to WT mice. These results model clinical observations that patients with pre-existing anti-tumor immune responses are more likely to respond to IT (50). Although the intrinsic tumor immunogenicity has often been invoked to explain these responses, focusing on the “immunological” make-up of the host may be important for an improved understanding of the determinants of response to IT.

Supplementary Material

Refer to Web version on PubMed Central for supplementary material.

ACKNOWLEDGEMENTS

We thank M. Taniguchi for providing iNKT−/− mice, and J. P. Allison for providing 9H10 antibody. We thank Alan B. Frey and James P. Allison for helpful comments about the manuscript.

This work was supported by Research Scholar award RSG-05-145-01-LIB from the American Cancer Society, NIH R01 CA113851, and by grants from The Chemotherapy Foundation and Elsa U. Pardee Foundation, all to S. Demaria.

REFERENCES

1. Rosenberg SA. Progress in human tumour immunology and immunotherapy. Nature 2001;411:380–384. [PubMed: 11357146]
2. Herber DL, Nagaraj S, Djeu JY, Gabrilovich DI. Mechanism and therapeutic reversal of immune suppression in cancer. Cancer Res 2007;67:5067–5069. [PubMed: 17545581]
3. Finn OJ. Cancer vaccines: between the idea and the reality. Nat Rev Immunol 2003;3:630–641. [PubMed: 12974478]
4. Gabrilovich DI, Bronte V, Chen SH, et al. The terminology issue for myeloid-derived suppressor cells. Cancer Res 2007;67:425. [PubMed: 17210725]
5. Salvadori S, Martinelli G, Zier K. Resection of solid tumors reverses T cell defects and restores protective immunity. J Immunol 2000;164:2214–2220. [PubMed: 10657677]
6. Shimizu J, Yamazaki S, Sakaguchi S. Induction of tumor immunity by removing CD25+CD4+ T cells: a common basis between tumor immunity and autoimmunity. J Immunol 1999;163:5211–5218. [PubMed: 10553041]
7. Bluestone JA, Abbas AK. Natural versus adaptive regulatory T cells. Nat Rev Immunol 2003;3:253–257. [PubMed: 12658273]
8. Liu VC, Wong LY, Jang T, et al. Tumor evasion of the immune system by converting CD4+CD25− T cells into CD4+CD25+ T regulatory cells: role of tumor-derived TGF-b. J Immunol 2007;178:2883–2892. [PubMed: 17312132]
9. Valzasina B, Piconese S, Guiducci C, Colombo MP. Tumor-induced expansion of regulatory T cells by conversion of CD4+CD25− lymphocytes is thymus and proliferation independent. Cancer Res 2006;66:4488–4495. [PubMed: 16618776]
10. Godfrey DI, Kronenberg M. Going both ways: immune regulation via CD1d-dependent NKT cells. J Clin Invest 2004;114:1379–1388. [PubMed: 15545985]
11. Van Kaer L. Alpha-Galactosylceramide therapy for autoimmune diseases: prospects and obstacles. Nat Rev Immunol 2005;5:31–42. [PubMed: 15630427]
12. Palmer JL, Tulley JM, Kovacs EJ, Gamelli RL, Taniguchi M, Faunce DE. Injury-induced suppression of effector T cell immunity requires CD1d-positive APCs and CD1d-restricted NKT cells. J Immunol 2006;177:92–99. [PubMed: 16785503]
13. Godfrey DI, MacDonald HR, Kronenberg M, Smyth MJ, Van Kaer L. NKT cells: what's in a name? Nat Rev Immunol 2004;4:231–237. [PubMed: 15039760]
14. Smyth MJ, Thia KY, Street SE, et al. Differential tumor surveillance by natural killer (NK) and NKT cells. J Exp Med 2000;191:661–668. [PubMed: 10684858]
15. Crowe NY, Smyth MJ, Godfrey DI. A critical role for natural killer T cells in immunosurveillance of methylcholanthrene-induced sarcomas. J Exp Med 2002;196:119–127. [PubMed: 12093876]
16. Terabe M, Matsui S, Noben-Trauth N, et al. NKT cell-mediated repression of tumor immunosurveillance by IL-13 and the IL-4R-STAT6 pathway. Nat Immunol 2000;1:515–520. [PubMed: 11101874]
17. Moodycliffe AM, Nghiem D, Clydesdale G, Ullrich SE. Immune suppression and skin cancer development: regulation by NKT cells. Nat Immunol 2000;1:521–525. [PubMed: 11101875]
18. Terabe M, Swann J, Ambrosino E, et al. A nonclassical non-V⟨14J⟨18 CD1d-restricted (type II) NKT cell is sufficient for down-regulation of tumor immunosurveillance. J Exp Med 2005;202:1627–1633. [PubMed: 16365146]
19. Terabe M, Matsui S, Park JM, et al. Transforming growth factor-β production and myeloid cells are an effector mechanism through which CD1d-restricted T cells block cytotoxic T lymphocyte-mediated tumor immunosurveillance: abrogation prevents tumor recurrence. J Exp Med 2003;198:1741–1752. [PubMed: 14657224]
20. Park JM, Terabe M, van den Broeke LT, Donaldson DD, Berzofsky JA. Unmasking immunosurveillance against a syngeneic colon cancer by elimination of CD4+ NKT regulatory cells and IL-13. Int J Cancer 2005;114:80–87. [PubMed: 15523692]

21. Ostrand-Rosenberg S, Clements VK, Terabe M, Park JM, Berzofsky JA, Dissanayake SK. Resistance to metastatic disease in STAT6-deficient mice requires hemopoietic and nonhemopoietic cells and is IFN-© dependent. J Immunol 2002;169:5796–5804. [PubMed: 12421960]
22. Terabe M, Khanna C, Bose S, et al. CD1d-restricted natural killer T cells can down-regulate tumor immunosurveillance independent of interleukin-4 receptor-signal transducer and activator of transcription 6 or transforming growth factor-beta. Cancer Res 2006;66:3869–3875. [PubMed: 16585215]
23. Hayakawa Y, Godfrey DI, Smyth MJ. Alpha-galactosylceramide: potential immunomodulatory activity and future application. Curr Med Chem 2004;11:241–252. [PubMed: 14754420]
24. Swann JB, Coquet JM, Smyth MJ, Godfrey DI. CD1-restricted T cells and tumor immunity. Curr Top Microbiol Immunol 2007;314:293–323. [PubMed: 17593666]
25. Demaria S, Bhardwaj N, McBride WH, Formenti SC. Combining radiotherapy and immunotherapy: a revived partnership. Int J Radiat Oncol Biol Phys 2005;63:655–666. [PubMed: 16199306]
26. Demaria S, Formenti SC. Sensors of ionizing radiation effects on the immunological microenvironment of cancer. Int J Radiat Biol 2007;83:819–825. [PubMed: 17852561]
27. Aslakson CJ, Miller FR. Selective events in the metastatic process defined by analysis of the sequential dissemination of subpopulations of a mouse mammary tumor. Cancer Res 1992;52:1399–1405. [PubMed: 1540948]
28. Demaria S, Kawashima N, Yang AM, et al. Immune-mediated inhibition of metastases following treatment with local radiation and CTLA-4 blockade in a mouse model of breast cancer. Clin Cancer Res 2005;11:728–734. [PubMed: 15701862]
29. Cui J, Shin T, Kawano T, et al. Requirement for Vα14 NKT cells in IL-12-mediated rejection of tumors. Science 1997;278:1623–1626. [PubMed: 9374462]
30. Kim KJ, Kanellopoulos-Langevin C, Merwin RM, Sachs DH, Asofsky R. Establishment and characterization of BALB/c lymphoma lines with B cell properties. J Immunol 1979;122:549–554. [PubMed: 310843]
31. Liu Y, Goff RD, Zhou D, et al. A modified alpha-galactosyl ceramide for staining and stimulating natural killer T cells. J Immunol Methods 2006;312:34–39. [PubMed: 16647712]
32. Matsumura S, Wang B, Kawashima N, et al. Radiation-induced CXCL16 release by breast cancer cells attracts effector T cells. J Immunol 2008;181:3099–3107. [PubMed: 18713980]
33. Tulley JM, Palmer JL, Gamelli RL, Faunce DE. Prevention of injury-induced suppression of T-cell immunity by the CD1d/NKT cell-specific ligand alpha-galactosylceramide. Shock 2008;29:269–277. [PubMed: 17693934]
34. Gallina G, Dolcetti L, Serafini P, et al. Tumors induce a subset of inflammatory monocytes with immunosuppressive activity on CD8+ T cells. J Clin Invest 2006;116:2777–2790. [PubMed: 17016559]
35. Gorelik E. Concomitant tumor immunity and the resistance to a second tumor challenge. Adv Cancer Res 1983;39:71–120. [PubMed: 6194674]
36. Dunn GP, Bruce AT, Ikeda H, Old LJ, Schreiber RD. Cancer immunoediting: from immunosurveillance to tumor escape. Nature Immunol 2002;3:991–998. [PubMed: 12407406]
37. Turk MJ, Guevara-Patiño JA, Rizzuto GA, Engelhorn ME, Sakaguchi S, Houghton AN. Concomitant tumor immunity to a poorly immunogenic melanoma is prevented by regulatory T cells. J Exp Med 2004;200:771–782. [PubMed: 15381730]
38. Matzinger P. Tolerance, danger, and the extended family. Annu Rev Immunol 1994;12:991–1045. [PubMed: 8011301]
39. Frey AB, Monu N. Effector-phase tolerance: another mechanism of how cancer escapes antitumor immune response. J Leukoc Biol 2006;79:652–662. [PubMed: 16415165]
40. Zhang B, Bowerman NA, Salama JK, et al. Induced sensitization of tumor stroma leads to eradication of established cancer by T cells. J Exp Med 2007;204:49–55. [PubMed: 17210731]
41. Egen JG, Kuhns MS, Allison JP. CTLA-4: new insights into its biological function and use in tumor immunotherapy. Nat Immunol 2002;3:611–618. [PubMed: 12087419]
42. Peggs KS, Quezada SA, Korman AJ, Allison JP. Principles and use of anti-CTLA4 antibody in human cancer immunotherapy. Curr Opin Immunol 2006;18:206–213. [PubMed: 16464564]

43. Sinha P, Clements VK, Ostrand-Rosenberg S. Reduction of myeloid-derived suppressor cells and induction of M1 macrophages facilitate the rejection of established metastatic disease. J Immunol 2005;174:636–645. [PubMed: 15634881]
44. Kusmartsev S, Gabrilovich DI. STAT1 signaling regulates tumor-associated macrophage-mediated T cell deletion. J Immunol 2005;174:4880–4891. [PubMed: 15814715]
45. Teng MW, Westwood JA, Darcy PK, et al. Combined natural killer T-cell based immunotherapy eradicates established tumors in mice. Cancer Res 2007;67:7495–7504. [PubMed: 17671220]
46. Wu DY, Segal NH, Sidobre S, Kronenberg M, Chapman PB. Cross-presentation of disialoganglioside GD3 to natural killer T cells. J Exp Med 2003;198:173–181. [PubMed: 12847141]
47. Scott-Browne JP, Matsuda JL, Mallevaey T, et al. Germline-encoded recognition of diverse glycolipids by natural killer T cells. Nat Immunol 2007;8:1105–1113. [PubMed: 17828267]
48. Shimizu K, Goto A, Fukui M, Taniguchi M, Fujii S. Tumor cells loaded with alpha-galactosylceramide induce innate NKT and NK cell-dependent resistance to tumor implantation in mice. J Immunol 2007;178:2853–2861. [PubMed: 17312129]
49. Jensen SM, Meijer SL, Kurt RA, Urba WJ, Hu HM, Fox BA. Regression of a mammary adenocarcinoma in STAT6−/− mice is dependent on the presence of STAT6-reactive T cells. J Immunol 2003;170:2014–2021. [PubMed: 12574371]
50. Speiser DE, Rimoldi D, Batard P, et al. Disease-driven T cell activation predicts immune responses to vaccination against melanoma. Cancer Immun 2003;3:12. [PubMed: 12962476]

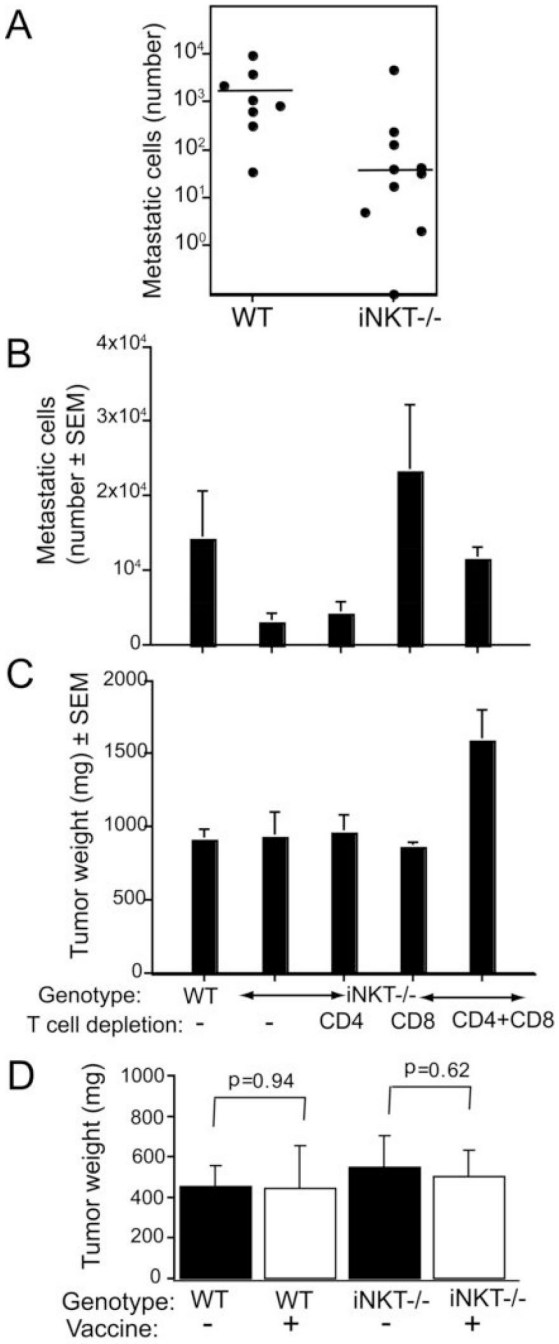

Figure 1. CD8 T cell-mediated inhibition of metastases in untreated tumor-bearing mice lacking iNKT cells

(A) Mice received 5×10^4 4T1 cells s.c. on Day 0. The number of metastatic cells in the lungs at Day 34 was significantly lower for the iNKT−/− than for the WT mice (p=0.0009). Each symbol represents one animal. (B, C) mAb-mediated CD4 and CD8 T-cell depletion was started on Day −1, and maintained up to the day of sacrifice. Mice were sacrificed on Day 33 to determine the tumor weigh (B) and number of metastatic cells in the lungs (C). Bars represent the mean ± SE of 8 to 10 animals/group. (B) There was no significant tumor weight difference (p>0.6) between WT and iNKT−/− mice non-depleted or depleted of CD8 or CD4 T cells. However, tumor weight was significantly increased in mice depleted of both T cell subsets

($p<0.01$ when compared to all other groups). (C) The number of metastases in iNKT−/− mice depleted of CD8 T cells (CD8) or CD4 and CD8 T cells (CD4+CD8) was significantly higher than in non-depleted iNKT−/− mice ($p=0.004$ and 0.001, respectively). In contrast, CD4 depletion did not significantly increase the number of metastases ($p=0.94$). Whereas there was a significant difference between WT and non-depleted iNKT−/− mice in the number of metastases ($p=0.043$), no significant difference was seen between WT and iNKT−/− mice after CD8 T cell depletion by itself or in combination with CD4 T cell depletion. (D) 4T1 cells are not intrinsically immunogenic in iNKT−/− mice. WT and iNKT−/− mice (N=5/group) were vaccinated weekly for 3 weeks with 10^6 irradiated (100 Gy) 4T1 cells s.c. in the left flank (+) or mock vaccinated with DMEM (−). Seven days after the last vaccination mice were challenged with 5×10^4 viable 4T1 cells and followed for tumor development. All mice developed tumors and there was significant difference in tumor weight in vaccinated WT ($p=0.94$) or iNKT ($p=0.62$) mice on Day 26.

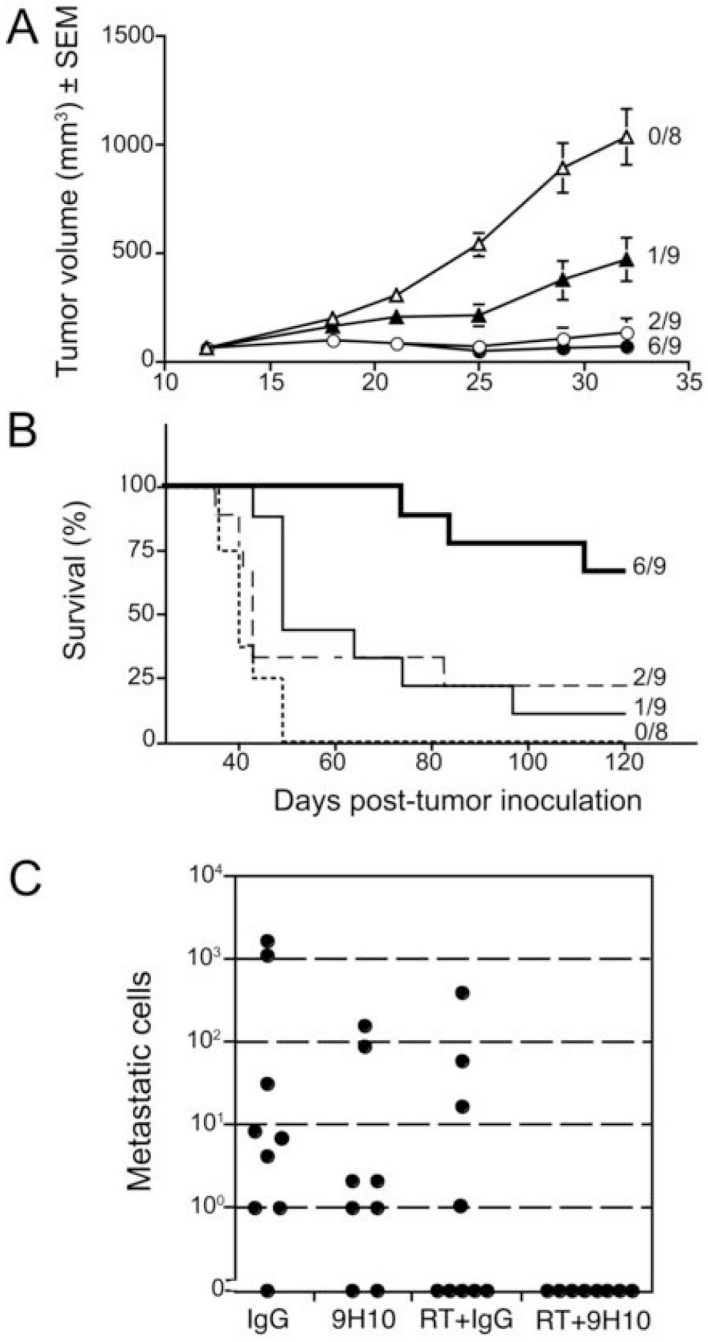

Figure 2. Therapeutic response of iNKT−/− mice with established 4T1 carcinoma to treatment with local RT and CTLA-4 blockade

Treatment was started on Day 13 post-s.c. inoculation with 4T1 cells. RT was delivered in two fractions of 12 Gy to the s.c. tumors on Day 13 and 14. Ab were given i.p. 1, 4 and 7 days post-RT. (A) Tumor growth delay in iNKT−/− mice treated with control hamster IgG (IgG) (open traingles, N=8), 9H10 (closed triangles, N=9), RT + IgG (open circles, N=9), or RT + 9H10 (closed circles, N=9). Tumor volume is shown as the mean ± SE for animals with tumors in each treatment group up to Day 32 when all animals were alive. The number of mice with complete tumor regression over the total number of mice per group is indicated. Tumor volume differences between treated and control (IgG) mice were statistically significant ($p<0.05$) from

Day 18 for RT and RT+9H10 groups, and from Day 21 for 9H10 group. (B) Percentage of surviving mice following treatment with control hamster IgG (IgG) (broken line, N=8), 9H10 (thin line, N=9), RT + IgG (dashed line, N=9), or RT + 9H10 (bold line, N=9). The number of mice surviving and tumor-free up to Day 121 over the total number of mice per group is indicated. Treatment with RT+9H10 ($p<0.0001$) and 9H10 ($p=0.002$) resulted in a statistically significant improvement in overall survival as compared to control (IgG) mice, whereas treatment with RT alone did not ($p=0.16$). (C) Number of metastatic cells in the lungs of iNKT −/− mice at Day 35 post subcutaneous tumor inoculation. Each symbol represents a single animal. Treatment groups are as above. Relative to control (IgG) mice, the number of metastases was significantly lower in RT+9H10 ($p=0.004$) group but not in RT+IgG ($p=0.15$) and 9H10 ($p=0.3$) groups.

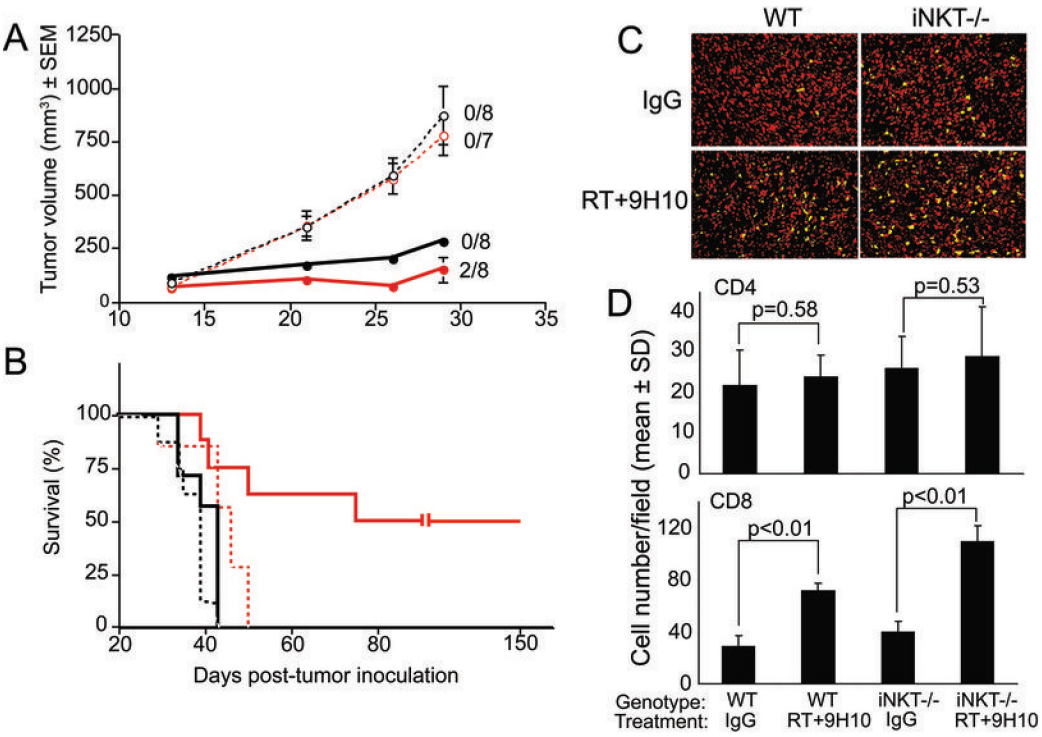

Figure 3. Comparison between WT and iNKT−/− mice with established 4T1 carcinoma in the response to treatment with local RT and CTLA-4 blockade

Comparison of response to treatment with RT and 9H10 (solid lines) or IgG (broken lines) in WT (black) and iNKT−/− (red) 4T1-tumor bearing mice. Treatment was started on Day 13 post-s.c. inoculation in the flank. RT was delivered in two fractions of 12 Gy to the s.c. tumors on Day 13 and 14. Ab were given i.p. 1, 4 and 7 days post-RT. (A) Tumor volume is shown as the mean ± SE for animals with tumors in each treatment group up to Day 29 when all animals were alive. The number of mice with complete tumor regression by Day 29 over the total number of mice per group is indicated. Two additional iNKT−/− mice had complete tumor regression after Day 29. Primary tumor growth was not significantly different in WT and iNKT −/− mice receiving the control IgG ($p>0.05$) at all time points. In contrast, iNKT−/− mice receiving RT+9H10 had a significantly lower tumor volume than WT mice receiving RT+9H10 ($p<0.05$) from Day 21. Tumor volume differences between RT+9H10 and control (IgG) mice were statistically significant ($p<0.05$) from Day 21 within each genotype. (B) Data are shown as the percentage of surviving mice over time. Surviving tumor-free mice were followed up to Day 150. iNKT mice treated with RT+9H10 showed a statistically significant improvement in overall survival ($p<0.05$) as compared to all other groups. Half of the iNKT−/− mice but none of the WT mice were cured from established 4T1 tumors by treatment with RT and CTLA-4 blockade. (C, D) In a separate group of mice treated as above, tumors were excised at Day 29 and analyzed by fluorescence microscopy for the presence of CD4+ and CD8+ T cells. (C) Representative fields showing CD8+ T cells (green) infiltrating 4T1 tumors in WT and iNKT −/− mice treated as indicated. Nuclei were stained with DAPI (red). (D) Mean numbers of CD4 + and CD8+ TILs in three mice per group. In both WT and iNKT−/− mice, CD8+ but not CD4 + TILs were increased by RT+9H10 treatment, but the increase was more pronounced in iNKT −/− mice ($p=0.006$).

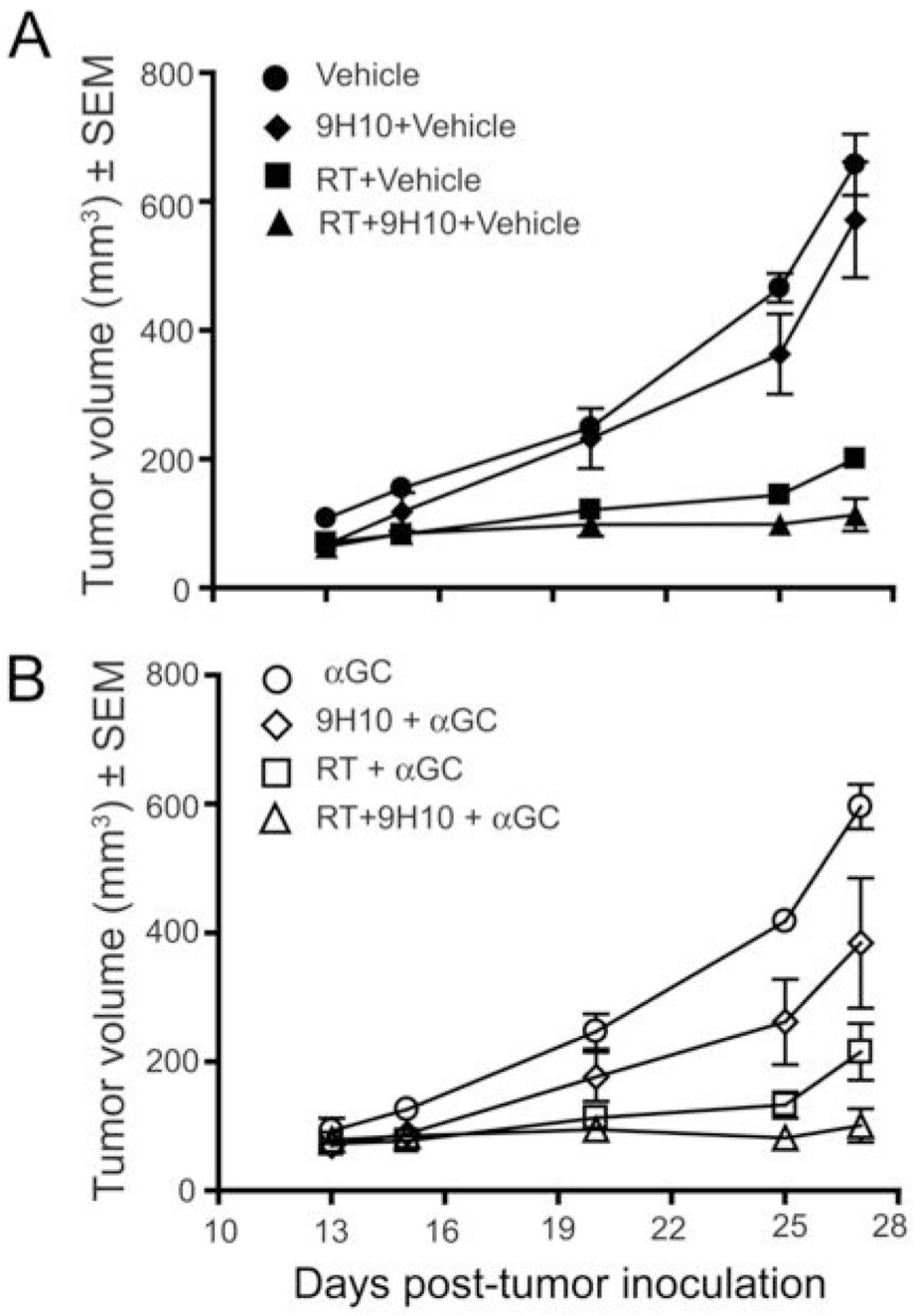

Figure 4. Administration of αGC does not enhance the response of 4T1 tumor-bearing WT mice to local RT and CTLA-4 blockade

Treatment was started on Day 13 post-s.c. inoculation in the flank. RT was delivered in two fractions of 12 Gy to the s.c. tumors on Day 13 and 14. 9H10 was given i.p. 1, 4 and 7 days post-RT. αGC (100 ng) was given i.p. twice per week starting on Day 1 post-RT. WT mice (N=5/group) were treated with (A) vehicle (closed circles), 9H10 + vehicle (closed diamonds), RT + vehicle (closed squares), RT + 9H10 + vehicle (closed triangles), (B) αGC (open circles), 9H10 + αGC (open diamonds), RT + αGC (open squares), or RT + 9H10 + αGC (open triangles). Tumor volume is shown as the mean ± SEM for animals with tumors in each treatment group up to Day 27 when all animals were alive. RT caused a significant ($p<0.001$

compared to control) tumor growth delay that was slightly enhanced by 9H10 but not by αGC. Although tumor volume differences between mice treated with αGC +9H10 and control were statistically significant (p=0.0396), the triple combination of αGC, RT and 9H10 did not show better tumor control than the combination of RT+9H10, and no complete tumor regression was observed.

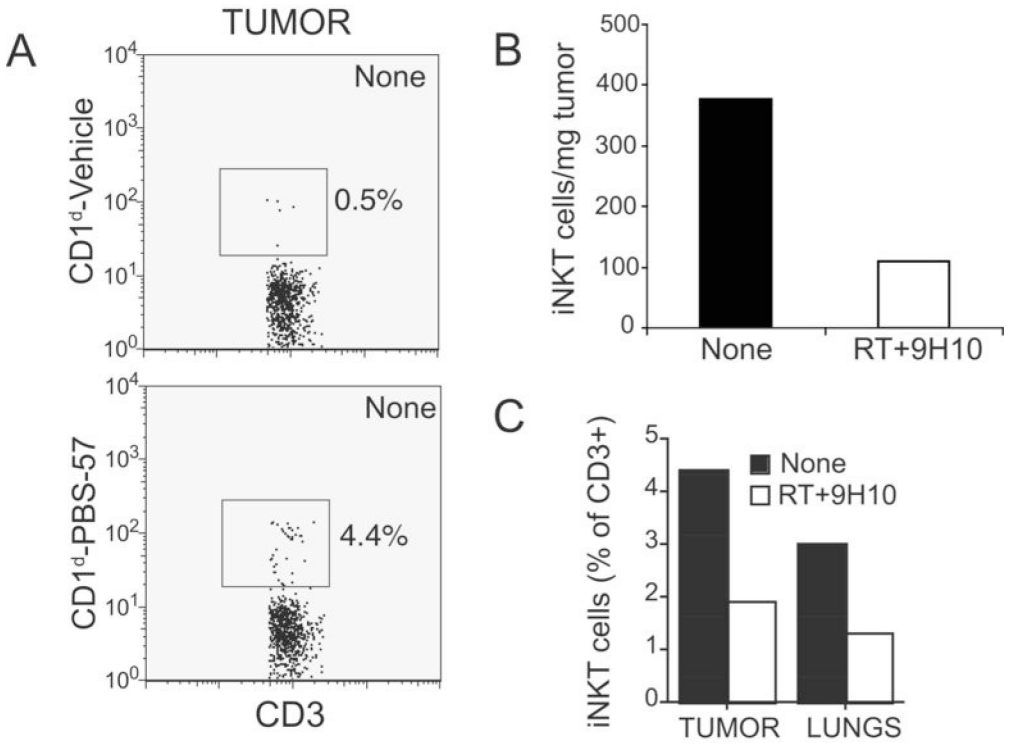

Figure 5. iNKT cells infiltrating 4T1 tumors are reduced by treatment with local RT and CTLA-4 blockade

WT mice were injected with 4T1 cells on Day 0 and left untreated (None) or treated with local RT and 9H10 (RT+9H10) as described in the legend of Figure 3. Tumors and lungs were harvested on Day 29, and obtained single cell suspensions stained FITC-anti-CD3 mAb and CD1d-PBS-57 PE or control CD1d-Vehicle PE tetramers to identify iNKT cells, followed by flow cytometry analysis. The lymphocyte gate was set based on the scattered plots in the spleen. (A) Histograms showing tumor-derived cells from untreated mice stained with CD3 and CD1d-PBS-57 or control tetramers, as indicated, and gated on CD3+ cells. Numbers indicate the percentage of cells in the square gate. (B) The percentage of cells in the lymphocyte gate positive for CD3 and CD1d-PBS-57 was multiplied for the percentage of cells in the lymphocyte gate and for the total number of viable cells isolated from the tumors, and divided for the tumor weight to obtain the number of cells per mg of tumor in treated (RT+9H10, white bar) and untreated (None, black bar) mice. (C) Percentage of CD3+ T cells that bind the CD1d-PBS-57 tetramers in tumor and lungs of treated (RT+9H10, white bars) and untreated (None, black bars) mice, as indicated. All data are from 4 to 5 mice of each group. Errors bars are absent because pooling of tumors and lungs within each group was necessary to obtain sufficient cells for analysis.

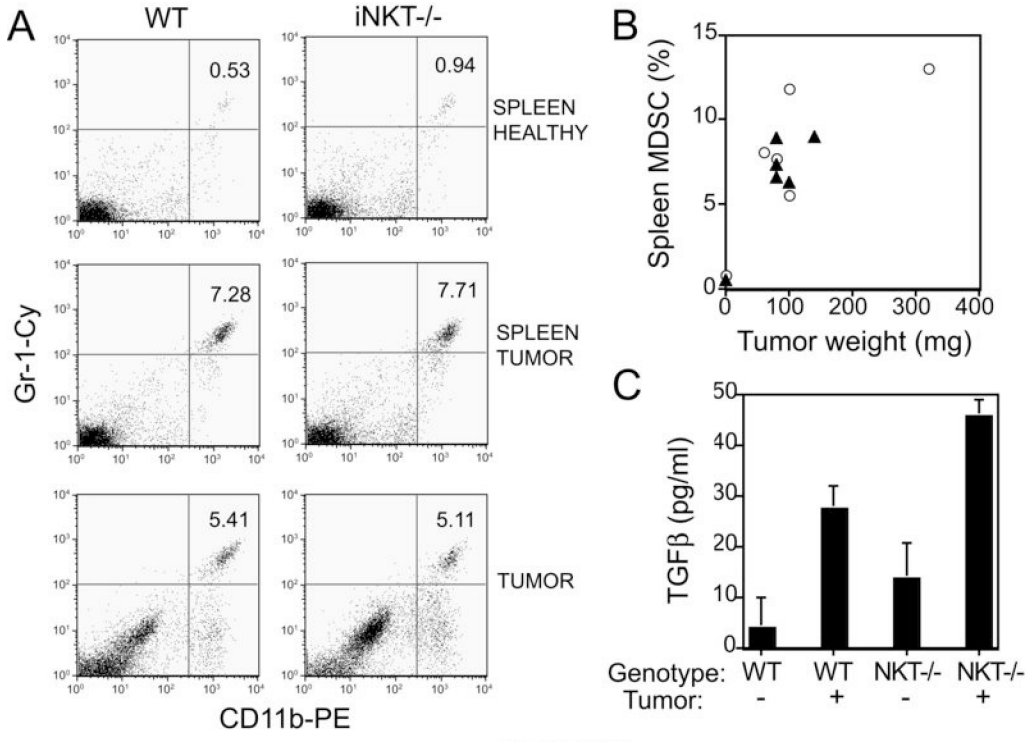

Figure 6. Accumulation of MDSC and TGFβ production in WT and iNKT−/− mice bearing 4T1 tumors

WT and NKT−/− mice were inoculated s.c. with 5×10^4 4T1 cells on Day 0 (N=5/group). 3 non-tumor-bearing mice of each genotype served as controls. On Day 14 primary tumors and spleens were harvested and obtained cell suspensions were stained with PE-anti-CD11b and Cy-anti-Gr-1 mAbs to detect MDSC. (A) Representative histograms of spleen from one healthy (top row) and one tumor-bearing (middle row) mouse showing the CD11b+Gr-1+ MDSC. Histograms from pooled tumors isolated from 5 WT and 5 iNKT−/− mice showing the CD11b +Gr-1+ MDSC (bottom row). Numbers indicate the percentage of MDSC. (B) Percentage of spleen MDSC in relation to the tumor weight in WT (closed triangles) and iNKT−/− (open circles) mice. Each symbol represents an individual mouse. For control healthy mice, one symbol representing the mean of 3 animals is shown. (C) Splenocytes isolated from tumor-free (−) (N=3) and tumor-bearing (+) (N=5) mice were cultured o.n. and the concentration of TGFβ in the culture supernatants was determined by ELISA. Data are the mean ± SE. In both WT and iNKT−/− mice spleen cells derived from tumor-bearing mice produced significantly more TGFβ than spleen cells derived from healthy mice ($p<0.05$). Although the baseline production of TGFβ did not differ significantly between WT and iNKT−/− healthy mice ($p=0.35$), tumor-bearing iNKT−/− mice produced more TGFβ than tumor-bearing WT mice ($p<0.01$).